Unmanned Systems, Vol. 14, No. 1 (2026) 215–226

DOI: 10.1142/S2301385025500906

Unmanned Systems
https://www.worldscientific.com/worldscinet/us

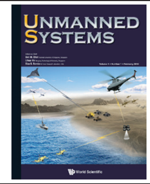

Control Approach for Disturbed Autonomous Helicopters Preserving Nonaffine and Non-Minimum Phase Characters

Hao Yang[*,‡], Haixiang Jiang[*], Hailong Pei[†], Xinpan Gou[*]

[*]*School of Automation, Guangdong Polytechnic Normal University, Guangzhou 510665, P. R. China*

[†]*Key Laboratory of Autonomous Systems and Networked Control, Ministry of Education,*
Unmanned Aerial Vehicle Systems Engineering Technology Research Center of Guangdong,
South China University of Technology, Guangzhou 510640, P. R. China

This paper addresses the importance of accounting for both nonaffine-in-control structure and non-minimum phase behavior in the control of autonomous unmanned helicopters (AUHs). Many existing control methods for AUHs tend to simplify these complexities. Such approximations can restrict operational regime, compromise flight performance, and potentially lead to system instability. To overcome these limitations, we introduce a feasible control strategy for 3-DOF AUHs that preserves these essential characteristics while also accounting for external disturbances. First, we construct an augmented fast subsystem to transform the closed-loop system into the standard singular perturbed form. Thereafter, we derive and manipulate the order-reduced subsystems separately in the fast and slow time-scales. In the fast time-scale, the flapping angle is exponentially stabilized around the desired manifold. In the slow time-scale, we transform AUHs into a simpler affine form compared to the original model through the manifold derived in the fast time-scale, and then an observer-based nonlinear controller is designed to guarantee the uniformly ultimately bounded stability of the resulting order-reduced slow subsystem. Finally, the tracking performance of the entire system is analyzed and ensured under the singular perturbation theory. To illustrate the effectiveness of our method, we present two simulation examples comparing our approach with existing methods using simplified models. The analysis of the results highlights the issues arising from these approximations, and demonstrates the superior performance of our proposed control method in terms of reduced amplitude of input, decreased setting time, and improved tracking accuracy.

Keywords: Autonomous unmanned helicopter; nonaffine; non-minimum phase; singular perturbation theory; disturbance-rejection; nonlinear dynamic inversion.

1. Introduction

During the past decades, unmanned aerial vehicles (UAVs) have found extensive applications in various fields, including scientific research, industrial tasks, agricultural activities, military operations, and more [1, 2]. Among the different types of UAVs, autonomous unmanned helicopters (AUHs) have garnered significant attention due to their exceptional maneuverability, agile movement, rapid response, and vertical take-off and landing capabilities [3]. However, the control design for AUHs poses substantial challenges in practical engineering due to their complex high-order dynamics, nonlinearity, strong coupling effects, and nonaffine-in-control structure [4].

Up to the present, researchers have proposed numerous sophisticated approaches to address various challenges related to AUHs. By applying approximate feedback linearization, Chen translated the model of AUH into a simplified form and designed a set of finite-time disturbance observers for AUHs in the presence of high-order disturbances [5]. Siri proposed a predictor-based control law through back-stepping procedure for AUHs with long input delays [6]. Learning-based adaptive control methods were widely applied to AUHs with unknown dynamics [7, 8]. However, the aforementioned controllers were built with the negligence of the strong non-minimum phase character

Received 5 July 2024; Accepted 14 November 2024; Published 18 June 2025. This paper was recommended for publication in its revised form by editorial board member, Wen-Hua Chen.
Email Address: ‡*yanghao@gpnu.edu.cn*

in AUHs, which arises from the coupling effect between the forces generated by cyclic pitch and the moments created by the flapping angle. As analyzed by Siddarth [9], the stabilization of inertial position may excite the periodic behavior in the pitch channel, and the error between the exact and approximated forces can exceed 100% in horizontal direction. Consequently, neglecting such coupling effects would severely limit the operational regime of AUHs. The development of advanced nonlinear controllers for AUHs while considering the non-minimum phase character has become a crucial research focus. Siddarth took advantage of the inherent three time-scale separation characteristic of helicopters to construct a composite controller. Recently, the inherent time-scale was proved to be unreliable during forward flight, and state extension was implemented with time-scale assignment to achieve exponential tracking performance with retained non-minimum phase behavior [10]. By means of time-varying gain extended state observer and neural networks (NN), Yan developed an adaptive dynamic programming controller for disturbed AUHs [11].

However, the control methods mentioned above approximate the dynamic model of AUHs to be affine-in-control. Consider the longitudinal direction. The flapping angle "a" of the main rotor was assumed to be sufficiently small, allowing the approximations $\sin(a) \approx a$ and $\cos(a) \approx 1$. These approximations transform the nonaffine structure into an affine form, which is essential for deriving the explicit inversion needed for controller design. As pointed out by Seo [4, 12], such assumptions can impose limitations on the applicable conditions and significantly degrade flight performance. In Sec. 2.2, we will present a simulation example to analyze the impact of ignoring the nonaffine structure of AUH. To deal with the nonaffine structure of AUHs, some researchers have investigated NN and fuzzy logic (FL)-based adaptive control methods. Tee [13] utilized NN to approximate unknown functions, and designed an adaptive nonaffine controller for AUHs in vertical flight. Dynamic approximation technique was adopted with FL-based adaptive controller for the nonaffine yaw channel model of AUHs with uncertainties [14]. Zhang [15] transformed the nonaffine model into an affine form, and then developed an NN-based flight controller. Nevertheless, the implementation of intelligent strategies may cause issues such as high computational burden, degraded control performance, or even instability, impacting their practical applicability [4, 16, 17].

Hovakimyan [18] proposed a singular perturbation theory (SPT)-based control strategy, known as approximate dynamic inversion (ADI), for a class of nonaffine nonlinear systems. Owing to its feasibility, a large number of relevant control methods have been developed [19, 20]. Recently, Seo adopted ADI to establish a multi-time-scale structure for nonaffine AUH to achieve robust and predictive control performance [4, 12]. Despite considering the nonaffine structure, the methods in [4, 12] ignored the non-minimum phase character. To the best of our knowledge, the control problems of AUHs incorporating both non-minimum phase behavior and nonaffine structure remain largely unexplored.

Motivated by the aforementioned circumstances, this paper proposes a feasible tracking control strategy for disturbed 3-DOF AUHs that retaining both nonaffine structure and non-minimum phase behavior. We first construct an augmented fast subsystem so that the entire system can be reformulated in the standard singular perturbed form (SSPF). Subsequently, two order-reduced subsystems are derived based on SPT in fast and slow time-scales. In the fast time-scale, the flapping angle dynamics are designed to converge exponentially toward the desired manifold. In the slow time-scale, we transform the original model of AUHs into an affine form. Thereafter, a nonlinear observer-based controller is built such that the resulting slow subsystem achieves uniformly ultimately bounded (UUB) stability under external disturbances. At last, the tracking performance of closed-loop system is ensured by SPT. The main contributions of the proposed strategy are as follows:

- In contrast to prior research [4, 9, 10, 12], the controller developed in this paper is designed without any approximations regarding the nonaffine-in-control structure and the non-minimum phase character. Furthermore, it effectively accounts for the presence of disturbances. These advancements contribute to a wider operating range and significantly improved flying performance.
- Unlike the SPT-based controller presented in [9, 10], the effectiveness of our method is not constrained by the inherent time-scale characteristics of AUHs. This independence highlights its feasibility and potential for broader application.

This paper is arranged as follows. Section 2 provides an overview of SPT and formulates the problem. Section 3 presents the detailed controller design strategy. Section 4 introduces the main theorem. The simulation results are presented in Sec. 5. Finally, Sec. 6 concludes.

2. Preliminaries and Problem Formulation

2.1. *Preliminaries on singular perturbation theory*

The mathematical foundation of SPT utilized in this paper will be briefly presented in this section. Consider the singular perturbation problem as follows [21]:

$$\begin{aligned} \dot{x} &= f(t,x,z,\epsilon_f), \\ \epsilon_f \dot{z} &= g(t,x,z,\epsilon_f), \end{aligned} \tag{1}$$

where $x \in D_x$, $z \in D_z$, $D_x \subset R^n$, and $D_z \subset R^m$; f and g are continuously differentiable in their arguments; $0 < \epsilon_f \ll 1$ is a small positive parameter characterizing time-scale split. The system (1) is in SSPF, if $0 = g(t,x,z,\epsilon_f)$ has $k \geq 1$ isolated real roots $z = h_i(t,x)$, $i = 1,\ldots,k$. For ease of notation, we fix an i within the range 1 to k and omit the subscript from h_i hereafter. Denote $e = z - h(t,x)$ and $\tau_f = \frac{t}{\epsilon_f}$. By substituting $\epsilon_f = 0$, the "reduced slow subsystem" (RSS) and the "boundary-layer subsystem" (BLS) are derived, respectively, as follows:

$$\dot{x} = f(t,x,h(t,x),0), \tag{2}$$

and

$$\frac{de}{d\tau_f} = g(t,x,e+h(t,x),0). \tag{3}$$

Lemma 1 ([21, Theorems 11.1 and 11.2]). *Consider the singular perturbation problem described by (1), and let $z = h(t,x)$ be an isolated root of $0 = g(t,x,z,0)$. Suppose that the following conditions are satisfied for all $(t,x,z-h(t,x),\epsilon_f) \in [0,t_1] \times D_x \times D_e \times [0,\epsilon_{f0}]$ for $t_1 \in (0,\infty)$,*

- (A1) *The first partial derivatives of f and g with respect to (x,z,ϵ_f), and the first partial derivative of g with respect to t are continuous; the function $h(t,x)$ and $[\partial g(t,x,z,0)/\partial z]$ have continuous first partial derivatives with respect to their arguments.*
- (A2) *The reduced problem (2) has a unique solution $x_s(t) \in S$, for $t \in [t_0,t_1]$, where S is a compact subset of D_x.*
- (A3) *The origin is an exponentially stable equilibrium point of the BLS (3), uniformly in (t,x). Let $R_e \subset D_e$ be the region of attraction of (3), and Ω_e be a compact subset of R_x.*

Then there exists a positive constant $\epsilon_f^* > 0$, such that for all $t_1 > t_0$, $z_0 - h(t_0,x_0) \in \Omega_e$, and $0 < \epsilon_f \leq \epsilon_f^*$, the system (1) has a unique solution $x(t,\epsilon_f)$, $z(t,\epsilon_f)$ on $[t_0,t_1]$, and

$$\begin{aligned} x(t) &= x_s(t) + O(\epsilon_f), \\ z(t) &= h(t,x_s) + e(\tau_f) + O(\epsilon_f), \end{aligned} \tag{4}$$

hold uniformly for $t \in [t_b,t_1]$, where $O(\cdot)$ denotes the order of magnitude notation.

The Assumption (A3) in Lemma 1 can be verified by the following lemma.

Lemma 2 ([21, Definition 11.1, Chap. 11]). *The equilibrium point $e = 0$ of the BLS (3) is exponentially stable, uniformly in $(t,x) \in [0,\infty) \times D_x$, if the Jacobian matrix $[\partial g/\partial e]$ satisfies the eigenvalue condition*

$$\mathrm{Re}\left[\lambda\left\{\frac{\partial g}{\partial e}(t,x,h(t,x),0)\right\}\right] \leq -c < 0, \tag{5}$$

for all $(t,x) \in [0,\infty) \times D_x$, where $\lambda(\cdot)$ represents the eigenvalue of the matrix, and $c > 0$ is a positive constant.

2.2. *Problem formulation and control objective*

In this paper, the following model of a 3-DOF symmetric helicopter, in which the lateral and directional dynamics are in equilibrium, is considered [9, 10]:

$$\begin{bmatrix} \dot{x} \\ \dot{z} \end{bmatrix} = \begin{bmatrix} \cos\theta & \sin\theta \\ -\sin\theta & \cos\theta \end{bmatrix} \begin{bmatrix} u \\ w \end{bmatrix}, \tag{6}$$

$$\begin{bmatrix} \dot{u} \\ \dot{w} \end{bmatrix} = \frac{1}{m}\begin{bmatrix} -mqw - T_M \sin a \\ mqu - T_M \cos a \end{bmatrix} + \begin{bmatrix} \cos\theta & -\sin\theta \\ \sin\theta & \cos\theta \end{bmatrix} \begin{bmatrix} 0 \\ g \end{bmatrix} + \begin{bmatrix} d_u \\ d_w \end{bmatrix}, \tag{7}$$

$$\dot{\theta} = q, \tag{8}$$

$$\dot{q} = \frac{1}{I_y}(M_a a + h_M \cdot T_M \sin a - l_M \cdot T_M \cos a - Q_T) + d_q, \tag{9}$$

$$y = [x,z]^T, \tag{10}$$

where $[x,z]^T$ represents the position state vector of AUH in the North–East-Down frame; $[u,w]^T$ denotes the velocity state vector in the body frame; θ denotes the pitch angle, and q is the pitch angular velocity; m denotes the mass of the helicopter, and g is the gravitational acceleration; T_M is the main rotor thrust, and a represents the flapping angle; Q_T is the tail rotor torque, M_a denotes the spring constant, and I_y is the pitch moment of inertia; h_M and l_M denote the distances between the main rotor and the center of gravity along the upward and forward directions, respectively; d_u, d_w, and d_q are disturbances of velocities u, w, and pitch angular rate q; y is the output.

Remark 1. It is worth noting that the 3-DOF helicopter model has been extensive researched for control design due to its ability to represent complex movements applicable to various fields, including agriculture, industry, and military [9, 10, 22]. Previous studies [9, 10, 22] have made significant contributions. However, this paper maintains both non-minimum phase character and nonaffine-in-control structure, which more accurately represents the nonlinear relationship between control inputs and system dynamics in real-world helicopter systems. Additionally, the

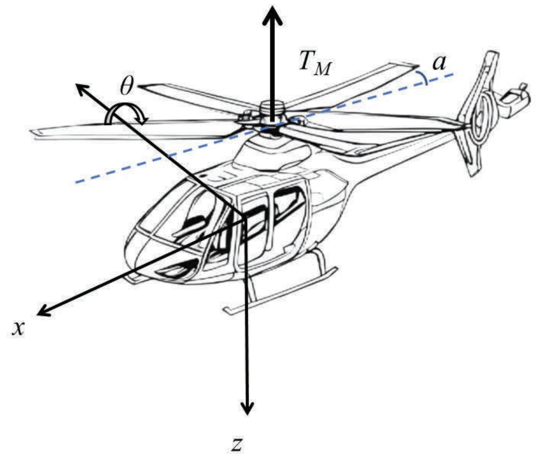

Fig. 1. View of 3-DOF AUHs.

model in (6)–(10) incorporates the influence of external disturbances, further enhancing its practical relevance.

The forces and moments of the thrust acting on AUH can be expressed as

$$\begin{aligned} F_x &= -T_M \sin a, \quad F_z = -T_M \cos a, \\ M_h &= -F_x \cdot h_M, \quad M_l = -F_z \cdot l_M. \end{aligned} \tag{11}$$

Referring to the internal dynamic analysis in [9], it was found that the exact and approximate forces acting on the AUHs exhibit a difference exceeding 100%. Although the control methods proposed in [9, 10] have taken the coupling effect into account, the nonaffine structure in (9) is simplified under the assumption of small values, resulting in the following approximations:

$$\begin{aligned} h_M \cdot T_M \sin a &\approx h_M \cdot T_M a, \\ l_M \cdot T_M \cos a &\approx l_M \cdot T_M. \end{aligned} \tag{12}$$

The impact of disregarding the non-minimum phase behavior has been investigated in [9]. To avoid redundant discussion, the details are omitted. Interested readers can refer to [9] for more information. Here, we will analyze the ramifications of simplification on nonaffine character in (12).

It can be observed from (11) and (12) that neglecting the nonaffine structure via the small angle assumption impacts the forces and moments on AUHs. Moreover, the error introduced by this simplification is exacerbated with increasing flapping angle. To illustrate this influence, we employ the controller in [9] for the nominal model of (6)–(10), in which the disturbances are not considered. The reference signals are $x_r = 0$, $z_r = 0$, the initial conditions and the parameters are borrowed from [9]: $x(0) = -2$m, $z(0) = 2$m, $u(0) = w(0) = 0$ m/s, $\theta(0) = 15$deg, $q(0) = 30$deg/s, $K_\theta = 3$, $K_q = 10$, $\alpha = \alpha_1 = 2$, $\beta = \beta_1 = 1$. We represent the forward and vertical positions as x_1 and z_1, respectively. The flapping angle is denoted as a_1.

Observe that although a_1 is within an acceptable region, there is a concerning negative vibration in the forward direction, which is dangerous for practical flight. Additionally, it takes 5 s for the helicopter to stabilize around the origin. To achieve better performance, we maintain the same initial conditions as before and adjust the tuning parameters as follows: $\alpha = 3$, $\alpha_1 = 8$, $\beta = 3$, $\beta_1 = 5$, $K_\theta = 20$, $K_q = 40$. The resulting responses are labeled as x_2, z_2, and a_2. As depicted in Fig. 2, the helicopter achieves faster stabilization in both directions without any negative vibration. However, the flapping angle a_2 reaches 120°, which is unacceptable for real application and exceeds the condition specified in the theory presented in [9] that flapping angle should be less than 30°. Although the nonaffine nonlinear control methods have been proposed for AUHs in [4, 12], the coupling effects in (7) have been ignored.

The aim of this paper is to present an SPT-based nonlinear control strategy for disturbed AUHs described by Eqs. (6)–(10) maintaining both the non-minimum phase character and the nonaffine structure such that the output y can successfully track the reference signal y_r. In order to facilitate the controller design, the following assumption and lemma are given.

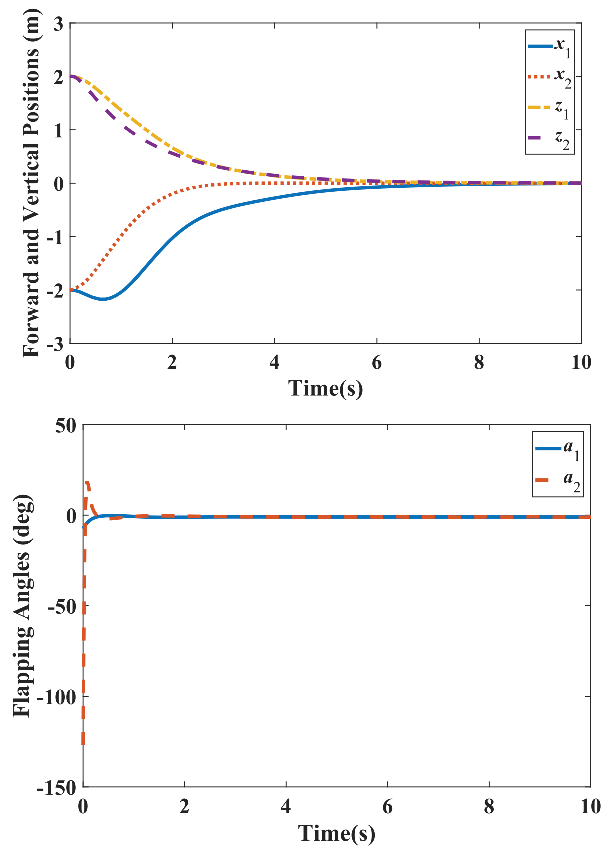

Fig. 2. Curves of positions and flapping angles.

Assumption 1. The disturbances and their first time derivatives are bounded as $|d_j| \leq d_i$ and $|\dot{d}_j| \leq \bar{d}_i$, where $d_i > 0$ and $\bar{d}_i > 0$ are positive constants for $i = 1, 2, 3$ and $j = u, w, q$.

Remark 2. In recent years, there has been a growing focus on control problems involving systems subject to disturbances described by Assumption 1 [23–25]. As highlighted in [23], the disturbances outlined in Assumption 1 are frequently encountered in practical applications, including cruise control in autonomous vehicles and voltage fluctuations in power systems.

Lemma 3 ([26, Lemma 3.2]). *For $x \in R, y \in R$, any positive real numbers p, q, b, and continuous function $a(\cdot) \geq 0$, the following inequality is hold:*

$$a(\cdot)x^p y^q \leq b|x|^{p+q} + \frac{q}{p+q}\left(\frac{p+q}{p}\right)^{-\frac{p}{q}} a(\cdot)^{\frac{p+q}{q}} b^{-\frac{p}{q}} |y|^{p+q}. \tag{13}$$

3. Controller Design and Main Result

3.1. *Fast augmented subsystem*

To introduce time-scale split, a fast augmented subsystem is designed as follows:

$$\begin{aligned} \varepsilon \dot{a} &= -\text{sign}\left(\frac{\partial Q}{\partial a}\right) Q, \\ Q &= \frac{1}{I_y}(M_a a + h_M T_M \sin a - l_M T_M \cos a - Q_T) - \nu. \end{aligned} \tag{14}$$

where $0 < \varepsilon \ll 1$ is a small tuning parameter, similar to the singular perturbation parameter ϵ_f in (1), and ν is the virtual controller, which will be designed later for the resulting RSS. By substituting (7), the second time derivative of $[x, z]^T$ can be derived as follows:

$$\begin{bmatrix} \ddot{x} \\ \ddot{z} \end{bmatrix} = -\frac{T_M}{m}\begin{bmatrix} \sin(\theta + a) \\ \cos(\theta + a) \end{bmatrix} + \begin{bmatrix} 0 \\ g \end{bmatrix} + \begin{bmatrix} \cos\theta & \sin\theta \\ -\sin\theta & \cos\theta \end{bmatrix}\begin{bmatrix} d_u \\ d_w \end{bmatrix}. \tag{15}$$

Then, the closed-loop system augmented with (14) can be given in the error-coordinate

$$\begin{aligned} \dot{e}_1 &= e_2, \\ \dot{e}_2 &= -\frac{T_M}{m}\begin{bmatrix} \sin(\theta + h_a) \\ \cos(\theta + h_a) \end{bmatrix} + \begin{bmatrix} 0 \\ g \end{bmatrix} - \begin{bmatrix} \ddot{x}_r \\ \ddot{z}_r \end{bmatrix} + \begin{bmatrix} \tilde{d}_u \\ \tilde{d}_w \end{bmatrix}, \\ \dot{\theta} &= q, \\ \dot{q} &= \frac{1}{I_y}(M_a a + h_M T_M \sin a - l_M T_M \cos a - Q_T) + d_q, \\ \varepsilon \dot{a} &= -\text{sign}\left(\frac{\partial Q}{\partial a}\right) Q, \end{aligned} \tag{16}$$

where $e_1 = [e_x, e_z]^T$, $e_x = x - x_r$, $e_z = z - z_r$, $\tilde{d}_u = d_u \cos\theta + d_w \sin\theta$, and $\tilde{d}_w = -d_u \sin\theta + d_w \cos\theta$. We assume the following assumptions are satisfied for (16).

Assumption 2. $[\partial Q / \partial a]$ is bounded away from zero, equivalently, it is either positive or negative.

Assumption 3. There is a solution $a = h_a$ such that $Q(h_a) = 0$.

Remark 3. The validity of Assumption 2 for ensuring the controllability of the system to employ ADI is supported by numerous studies [18–20, 27]. The existence of the smooth isolated root stated in Assumption 3 can be verified by [28, Lemma 1], which has been widely utilized in literature to demonstrate the existence of isolated roots in nonaffine nonlinear systems [23, 29, 30]. Additionally, both Assumptions 2 and 3 have been verified in real-world AUHs [4, 12] as well as in other applications [31].

According to SPT, the corresponding BLS and RSS can be derived as follows:

$$\frac{de_a}{d\tau} = -\text{sign}\left(\frac{\partial Q}{\partial a}\right) Q, \tag{17}$$

and

$$\begin{aligned} \dot{e}_1 &= e_2, \\ \dot{e}_2 &= -\frac{T_M}{m}\begin{bmatrix} \sin(\theta + h_a) \\ \cos(\theta + h_a) \end{bmatrix} + \begin{bmatrix} 0 \\ g \end{bmatrix} - \begin{bmatrix} \ddot{x}_r \\ \ddot{z}_r \end{bmatrix} + \begin{bmatrix} \tilde{d}_u \\ \tilde{d}_w \end{bmatrix}, \\ \dot{\theta} &= q, \\ \dot{q} &= \nu + d_q, \end{aligned} \tag{18}$$

where $\tau = t/\varepsilon$ represents the fast time-scale. In the next subsection, we will develop an observer-based nonlinear control law for the RSS in (18).

3.2. *Observer-based controller*

Design the following nonlinear observer to estimate disturbances:

$$\begin{aligned} \hat{d}_u &= \mu_1 + k_1 \dot{e}_x, \\ \dot{\mu}_1 &= -k_1 \mu_1 - k_1\left(k_1 \dot{e}_x - \frac{T_M}{m}\sin(\theta + h_a) - \ddot{x}_r\right), \\ \hat{d}_w &= \mu_2 + k_2 \dot{e}_z, \\ \dot{\mu}_2 &= -k_2 \mu_2 - k_2\left(k_2 \dot{e}_z - \frac{T_M}{m}\cos(\theta + h_a) + g - \ddot{z}_r\right), \\ \hat{d}_q &= -k_3(\mu_3 - q), \\ \dot{\mu}_3 &= \nu + \hat{d}_q, \end{aligned} \tag{19}$$

where μ_i are internal variables of observer, $\hat{d}_i$ are disturbance estimations, and k_i are the tuning gains, $i = 1, 2, 3$. Define estimation errors as $E_u = \hat{d}_u - \tilde{d}_u$, $E_w = \hat{d}_w - \tilde{d}_w$, and $E_q = \hat{d}_q - d_q$. Their time derivatives can be obtained as

$$\begin{aligned} \dot{E}_u &= -k_1 E_u - \dot{\tilde{d}}_u, \\ \dot{E}_w &= -k_2 E_w - \dot{\tilde{d}}_w, \\ \dot{E}_q &= -k_3 E_q - \dot{d}_q. \end{aligned} \tag{20}$$

Meanwhile, $\dot{\tilde{d}}_u$ and $\dot{\tilde{d}}_w$ are

$$\begin{aligned} \dot{\tilde{d}}_u &= -q d_u \sin\theta + \dot{d}_u \cos\theta + q d_w \cos\theta + \dot{d}_w \sin\theta, \\ \dot{\tilde{d}}_w &= -q d_u \cos\theta - \dot{d}_u \sin\theta - q d_w \sin\theta + \dot{d}_w \cos\theta. \end{aligned} \tag{21}$$

According to Assumption 1 and the expressions in (21), one achieves $\dot{\tilde{d}}_u \le \tilde{d}_1$ and $\dot{\tilde{d}}_w \le \tilde{d}_2$, where $\tilde{d}_1 > 0$ and $\tilde{d}_2 > 0$ are positive constants.

Introduce new variable $\xi_{1x} = e_x$, $\xi_{1z} = e_z$, $\xi_{2x} = \dot{e}_x + \sigma_x \xi_{1x}$, and $\xi_{2z} = \dot{e}_z + \sigma_z \xi_{1z}$, where $\sigma_x > 0$ and $\sigma_z > 0$ are positive parameters. Choose Lyapunov candidate $V_1 = \frac{1}{2}\xi_{1x}^2 + \frac{1}{2}\xi_{1z}^2$. Then, the time derivative of V_1 can be derived as

$$\dot{V}_1 = -\sigma_x \xi_{1x}^2 - \sigma_z \xi_{1z}^2 + \xi_{1x}\xi_{2x} + \xi_{1z}\xi_{2z}. \tag{22}$$

Denote $\theta_d = \theta - h_a$ as the desired value of pitch angle. The desired dynamics of e_x and e_z are designed as

$$\begin{aligned} \ddot{e}_{xd} &= -\alpha_x e_x - \beta_x \dot{e}_x - E_u \\ &= -\frac{T_M}{m}\sin(\theta_d + h_a) - \ddot{x}_r + \tilde{d}_u, \\ \ddot{e}_{zd} &= -\alpha_z e_z - \beta_z \dot{e}_z - E_w \\ &= -\frac{T_M}{m}\cos(\theta_d + h_a) + g - \ddot{z}_r + \tilde{d}_w, \end{aligned} \tag{23}$$

where $\alpha_x > 0$, $\alpha_z > 0$, $\beta_x > 0$, and $\beta_z > 0$ are some positive tuning parameters. By substituting $E_u = \hat{d}_u - \tilde{d}_u$ and $E_w = \hat{d}_w - \tilde{d}_w$, we obtain

$$\begin{aligned} &\ddot{x}_r - \alpha_x(1 - \beta_x)\xi_{1x} - \beta_x \xi_{2x} - \hat{d}_u = -\frac{T_M}{m}\sin(\theta_d + h_a), \\ &\ddot{z}_r - \alpha_z(1 - \beta_z)\xi_{1z} - \beta_z \xi_{2z} - \hat{d}_w - g = -\frac{T_M}{m}\cos(\theta_d + h_a). \end{aligned} \tag{24}$$

For brevity, we denote $\rho_1 = -\frac{T_M}{m}\sin(\theta_d + h_a)$ and $\rho_2 = -\frac{T_M}{m}\cos(\theta_d + h_a)$. Then, T_M and θ_d can be derived as follows:

$$T_M = m\sqrt{\rho_1^2 + \rho_2^2}, \quad \theta_d = \arctan\frac{\rho_1}{\rho_2} - h_a. \tag{25}$$

For this stage, we choose Lyapunov candidate as $V_2 = V_1 + \frac{1}{2}\xi_{2x}^2 + \frac{1}{2}\xi_{2z}^2 + \frac{1}{2}E_u^2 + \frac{1}{2}E_w^2$. By substituting (18) and (24), the time derivative of V_2 can be derived

$$\begin{aligned} \dot{V}_2 =\ & \dot{V}_1 + \xi_{2x}(\ddot{e}_x + \sigma\dot{\xi}_{1x}) + \xi_{2z}(\ddot{e}_z + \sigma\dot{\xi}_{1z}) + E_u\dot{E}_u \\ & + E_w\dot{E}_w \\ =\ & -\sigma_x\xi_{1x}^2 - \sigma_z\xi_{1z}^2 - (\beta_x - \sigma_x)\xi_{2x}^2 - (\beta_z - \sigma_z)\xi_{2z}^2 \\ & + (1 - \alpha_x - \sigma_x^2 + \beta_x\sigma_x)\xi_{1x}\xi_{2x} + (1 - \alpha_z - \sigma_z^2 \\ & + \beta_z\sigma_z)\xi_{1z}\xi_{2z} - \frac{T_M}{m}\xi_{2x}[\sin(\theta + h_a) - \sin(\theta_d \\ & + h_a)] - \frac{T_M}{m}\xi_{2z}[\cos(\theta + h_a) - \cos(\theta_d + h_a)] \\ & - \xi_{2x}E_u - \xi_{2z}E_w + E_u\dot{E}_u + E_w\dot{E}_w. \end{aligned} \tag{26}$$

According to Lemma 3, we have

$$\begin{aligned} l_x\xi_{1x}\xi_{2x} &\le \frac{1}{2}\xi_{1x}^2 + \frac{1}{2}l_x^2\xi_{2x}^2, \\ l_z\xi_{1z}\xi_{2z} &\le \frac{1}{2}\xi_{1z}^2 + \frac{1}{2}l_z^2\xi_{2z}^2, \\ -\xi_{2x}E_u &\le \frac{1}{2}\xi_{2x}^2 + \frac{1}{2}E_u^2, \\ -\xi_{2z}E_w &\le \frac{1}{2}\xi_{2z}^2 + \frac{1}{2}E_w^2, \end{aligned} \tag{27}$$

where $l_x = 1 - \alpha_x - \sigma_x^2 + \beta_x\sigma_x$ and $l_z = 1 - \alpha_z - \sigma_z^2 + \beta_z\sigma_z$. According to [21, Lemma 3.3], functions $\sin(\cdot)$ and $\cos(\cdot)$ are globally Lipschitz, which implies

$$\begin{aligned} -\frac{T_M}{m}\xi_{2x}[\sin(\theta + h_a) - \sin(\theta_d + h_a)] &\le \frac{T_M}{m}(\xi_{2x}^2 + e_\theta^2), \\ -\frac{T_M}{m}\xi_{2z}[\cos(\theta + h_a) - \cos(\theta_d + h_a)] &\le \frac{T_M}{m}(\xi_{2z}^2 + e_\theta^2). \end{aligned} \tag{28}$$

By substituting (27) and (28) back to (26), we have

$$\begin{aligned} \dot{V}_2 \le & -\left(\sigma_x - \frac{1}{2}\right)\xi_{1x}^2 - \left(\beta_x - \sigma_x - \frac{1}{2}l_x^2 - \frac{1}{2} - \frac{T_M}{m}\right)\xi_{2x}^2 \\ & - \left(\sigma_z - \frac{1}{2}\right)\xi_{1z}^2 - \left(\beta_z - \sigma_z - \frac{1}{2}l_z^2 - \frac{1}{2} - \frac{T_M}{m}\right)\xi_{2z}^2 \\ & + \frac{2T_M}{m}e_\theta^2 + \frac{1}{2}E_u^2 + \frac{1}{2}E_w^2 + E_u\dot{E}_u + E_w\dot{E}_w. \end{aligned} \tag{29}$$

Denote $q = e_q + q_d$, where q_d is the desired pitch angular rate. Choose Lyapunov function as $V(x) = V_2 + \frac{1}{2}e_\theta^2 + \frac{1}{2}e_q^2 + \frac{1}{2}E_q^2$. By substituting (20) and (21), we obtain

$$\begin{aligned} \dot{V}(x) \le & -\left(\sigma_x - \frac{1}{2}\right)\xi_{1x}^2 - \left(\beta_x - \sigma_x - \frac{1}{2}l_x^2 - \frac{1}{2} - \frac{T_M}{m}\right)\xi_{2x}^2 \\ & - \left(\sigma_z - \frac{1}{2}\right)\xi_{1z}^2 - \left(\beta_z - \sigma_z - \frac{1}{2}l_z^2 - \frac{1}{2} - \frac{T_M}{m}\right)\xi_{2z}^2 \\ & + \frac{2T_M}{m}e_\theta^2 + e_\theta(e_q + q_d - \dot{\theta}_d) + e_q(\nu + d_q - \dot{q}_d) \end{aligned}$$

$$- \left(k_1 - \frac{1}{2}\right)E_u^2 - \left(k_2 - \frac{1}{2}\right)E_w^2 - k_3 E_q^2 - E_u \dot{\tilde{d}}_u - E_w \dot{\tilde{d}}_w - E_q \dot{d}_q. \tag{30}$$

Similarly, based on Lemma 3 and Assumption 1, the following inequalities are satisfied:

$$\begin{aligned} -E_u \dot{\tilde{d}}_u &\le \frac{1}{2}E_u^2 + \frac{1}{2}\bar{d}_1^2, \\ -E_w \dot{\tilde{d}}_w &\le \frac{1}{2}E_w^2 + \frac{1}{2}\bar{d}_2^2, \\ -E_q \dot{\tilde{d}}_q &\le \frac{1}{2}E_q^2 + \frac{1}{2}\bar{d}_3^2. \end{aligned} \tag{31}$$

Then we can reformulate (30) as follows:

$$\begin{aligned} \dot{V}(x) \le & -\left(\sigma_x - \frac{1}{2}\right)\xi_{1x}^2 - \left(\beta_x - \sigma_x - \frac{1}{2}l_x^2 - \frac{1}{2} - \frac{T_M}{m}\right)\xi_{2x}^2 \\ & - \left(\sigma_z - \frac{1}{2}\right)\xi_{1z}^2 - \left(\beta_z - \sigma_z - \frac{1}{2}l_z^2 - \frac{1}{2} - \frac{T_M}{m}\right)\xi_{2z}^2 \\ & + \frac{2T_M}{m}e_\theta^2 + e_\theta(e_q + q_d - \dot{\theta}_d) + e_q(\nu + d_q - \dot{q}_d) \\ & - (k_1 - 1)E_u^2 - (k_2 - 1)E_w^2 - \left(k_3 - \frac{1}{2}\right)E_q^2 \\ & + \frac{1}{2}(\bar{d}_1^2 + \bar{d}_2^2 + \bar{d}_3^2). \end{aligned} \tag{32}$$

The desired angular rate and control law are designed as

$$\begin{aligned} q_d &= -k_\theta e_\theta + \dot{\theta}_d, \\ \nu &= -e_\theta + \dot{q}_d - k_q e_q - \hat{d}_q. \end{aligned} \tag{33}$$

This completes the controller design.

4. Main Result

The main result can be summarized from the following theorem.

Theorem 1. *Consider the disturbed nonaffine nonlinear AUHs in (6)–(10) satisfying Assumptions 1, 2, and 3. Then, under the observer-based controller designed in (19), (25), and (33), there exists a positive constant ε^* such that for all $0 < \varepsilon \le \varepsilon^*$, the tracking errors and all the other states are bounded for any finite-time interval.*

Proof. For the AUHs in the closed-loop form in (16), Assumption (A1) is indicated to be satisfied. Meanwhile, Assumption 3 directly fulfills Assumption (A2). Assumption (A3) is satisfied by Assumption 2 and Lemma 2 since

$$\operatorname{sign}\left(\frac{\partial Q}{\partial a}\right) \cdot \frac{\partial Q}{\partial a} > 0. \tag{34}$$

According to Lemma 1, the errors between state responses of closed-loop system and RSS can be less than $O(\varepsilon)$ as long as ε is small enough. Now, the theorem can be proved if all the signals of RSS in (18) is UUB. By substituting q_d and ν in (33), we have

$$\begin{aligned} \dot{V}(x) \le & -\left(\sigma_x - \frac{1}{2}\right)\xi_{1x}^2 - \left(\beta_x - \sigma_x - \frac{1}{2}l_x^2 - \frac{1}{2} - \frac{T_M}{m}\right) \\ & \times \xi_{2x}^2 - \left(\sigma_z - \frac{1}{2}\right)\xi_{1z}^2 - \left(\beta_z - \sigma_z - \frac{1}{2}l_z^2 - \frac{1}{2} \right. \\ & \left. - \frac{T_M}{m}\right)\xi_{2z}^2 - \left(k_\theta - \frac{2T_M}{m}\right)e_\theta^2 - \left(k_q - \frac{1}{2}\right)e_q^2 \\ & - (k_1 - 1)E_u^2 - (k_2 - 1)E_w^2 - (k_3 - 1)E_q^2 + \frac{1}{2} \\ & \times (\bar{d}_1^2 + \bar{d}_2^2 + \bar{d}_3^2). \end{aligned} \tag{35}$$

Define

$$\begin{aligned} \chi = 2\min\Bigg\{ & \left(\sigma_x - \frac{1}{2}\right), \left(\sigma_z - \frac{1}{2}\right), \left(k_\theta - \frac{2T_M}{m}\right), \\ & \left(\beta_x - \sigma_x - \frac{1}{2}l_x^2 - \frac{1}{2} - \frac{T_M}{m}\right), \\ & \left(\beta_z - \sigma_z - \frac{1}{2}l_z^2 - \frac{1}{2} - \frac{T_M}{m}\right), \\ & \left(k_q - \frac{1}{2}\right), (k_i - 1)\Bigg\}, \end{aligned} \tag{36}$$

and $\bar{d} = \frac{3}{2}\max\{\bar{d}_i\}$, $i = 1, 2, 3$. Then, we have

$$\dot{V} \le -\chi V + \bar{d}. \tag{37}$$

According to the Comparison Lemma in [21], we have

$$V \le V(t_0)e^{-\chi t} + \frac{\bar{d}}{\chi}. \tag{38}$$

Then, for any $0 < \rho < 1$, the following can be obtained:

$$V \le (1 + \rho)\frac{\bar{d}}{\chi}, \tag{39}$$

for $t \ge T$, where $T = \max\{t_0, \frac{1}{\chi}\ln(\frac{\chi V(t_0)}{\rho \bar{d}})\}$. According to [21, Definition 4.6], all the signals of RSS in (18) and observer in (19) are UUB. By applying Lemma 1, we have

$$|e_1| \le |e_{1s}| + |O(\varepsilon)|, \tag{40}$$

where e_1 and e_{1s} are the tracking error vectors of closed-loop system in (16) and RSS in (18), respectively. This completes the proof. □

Remark 4. As can be seen in (35), the parameters of the controller should be selected such that $(\sigma_x - \frac{1}{2})$, $(\sigma_z - \frac{1}{2})$, $(\beta_x - \sigma_x - \frac{1}{2}l_x^2 - \frac{1}{2} - \frac{T_M}{m})$, $(\beta_z - \sigma_z - \frac{1}{2}l_z^2 - \frac{1}{2} - \frac{T_M}{m})$, $(k_\theta - \frac{2T_M}{m})$, $(k_q - \frac{1}{2})$, $(k_i - 1)$ are positive. This implies that α_x and α_z

should be chosen such that l_x and l_z are sufficiently small. Furthermore, according to [32, Theorem 1], when the observer gains k_i are adjusted to positive values, the observer can effectively estimate the disturbances, $i = 1, 2, 3$. It is also important to note that, unlike the SPT-based control methods presented in [9, 10], the singular perturbation parameter $0 < \varepsilon \ll 1$ is independent of the AUH model. Therefore, we can select ε to be small enough to guarantee the effectiveness of time-scale decomposition and to reduce the tracking error in (40).

Remark 5. Similar to the work in [4, 12], the flight conditions of the AUH should be determined by the parameter tuning requirements outlined in Remark 4, the satisfaction of Assumption 2, and the mechanical constraints of the practical helicopter platform.

5. Simulation Results

In this section, two comparative examples are carried out to illustrate the effectiveness and tracking performance of the proposed control strategy. The AUH is the same as in [9, 10], and the values of the corresponding parameters can be found in Table 1. Substituting (14) into $[\partial Q/\partial a]$, we have

$$\begin{aligned}\frac{\partial Q}{\partial a} &= M_a + h_M \cdot T_M \cos a + l_M \cdot T_M \sin a \\ &= T_M \sqrt{h_M^2 + l_M^2} \sin(a + \phi) + M_a,\end{aligned}$$

$$\sin\phi = \frac{h_M}{\sqrt{h_M^2 + l_M^2}}, \quad \cos\phi = \frac{l_M}{\sqrt{h_M^2 + l_M^2}}, \tag{41}$$

According to the parameters of AUH there is a large operating region, in which the Assumption 2 is satisfied.

5.1. *Example 1*

In this example, to demonstrate the effectiveness of the proposed method, we will apply the provided control law to the hovering problem described in Sec. 2.2 with the same initial conditions. The simulation results will be compared with the controller from [9] with the second set of parameters in Sec. 2.2. The tuning parameters of our controller are: $\alpha_x = 3, \alpha_z = 8, \beta_x = 3, \beta_z = 5, k_\theta = 20, k_q = 40, k_1 = 0, k_2 = 0, k_3 = 0, \mu_1 = 0, \mu_2 = 0$. For ease of distinction, the simulation results under our controller are denoted by subscript "3".

The results in Fig. 3 indicate that neglecting the nonaffine structure leads to a significant increase in the amplitude of flapping angle to achieve desired performance. This observation aligns with the intuition that there is a discrepancy between the computational input, which ignores the nonaffine structure, and the actual control input required by AUHs. As a comparison, under our control scheme, the maximum flapping angle remains below 22°, and the setting time is reduced by about 50% in the vertical direction. Compared with the simulation results obtained under the controller from [9, Sec. 2.2], the control method in this paper achieves superior dynamic performance with a more feasible flapping angle by preserving the nonaffine structure of AUHs.

Table 1. Parameters of AUH.

Parameter	Value
m	4.9 kg
g	9.81 m/s^2
Q_T	0.0110 N · m
M_a	25.23 N · m/rad
I_y	0.271256 kg · m^2
h_M	0.2943 m
l_M	−0.015 m

5.2. *Example 2*

The following reference trajectories are considered in this example:

$$x_r(t) = \begin{cases} 0 & 0 \le t \le 2, \\ 5t - 10 & 2 \le t \le 7, \\ 25 & 7 \le t \le 12, \\ -5t + 85 & 12 \le t \le 17, \\ 0 & 17 \le t \le 25, \end{cases} \tag{42}$$

$$z_r(t) = \begin{cases} 5t & 0 \le t \le 2, \\ 10 & 2 \le t \le 17, \\ -4t + 78 & 17 \le t \le 19, \\ 2 & 19 \le t \le 25. \end{cases} \tag{43}$$

The external disturbances are set as $d_u = 0.5\cos t + 1$, $d_w = \cos t$, $d_q = \sin(2t) + 0.2\cos t$.

In order to verify the tracking performance of the proposed method, we will compare the simulation results with the prescribed performance controller (PPC) in [22], which is developed for 3-DOF helicopters with disturbances. The parameters of controller proposed in this paper are adjusted as: $\alpha_x = 3.5$, $\alpha_z = 8$, $\beta_x = 3$, $\beta_z = 5$, $k_\theta = 14$, $k_q = 80$, $k_1 = 400$, $k_2 = 400$, $k_3 = 200$, $\mu_1 = 10$, $\mu_2 = 10$. For PPC, the prescribed performance functions are selected as

$$\rho_i = (\rho_{i0} - \rho_{i\infty})e^{l_i t} + \rho_{i\infty}, \quad i = 1, \ldots, 4, \tag{44}$$

where $\rho_{10} = 10$, $\rho_{1\infty} = 0.8$, $\rho_{20} = 10$, $\rho_{2\infty} = 1.5$, $\rho_{30} = 10$, $\rho_{3\infty} = 0.5$, $\rho_{40} = 15$, $\rho_{4\infty} = 1$, $l_1 = -2$, $l_2 = -1.2$, $l_3 = -2$,

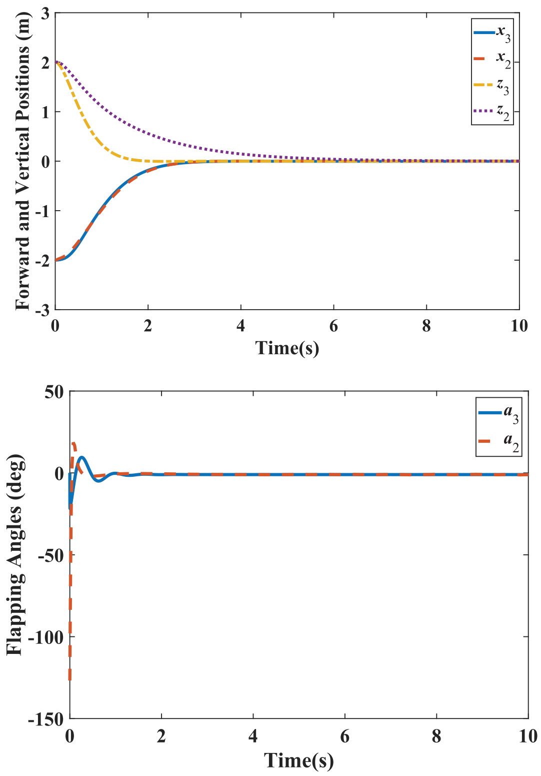

Fig. 3. Curves of positions and flapping angles.

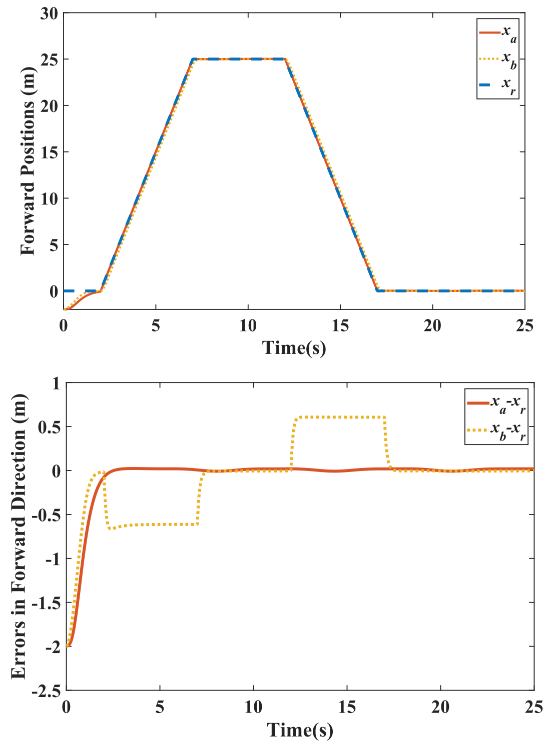

Fig. 4. Curves of forward positions and tracking errors.

$l_4 = -1.1$. The tuning parameters of PPC are chosen as: $k_1 = 4$, $k_2 = 200$, $k_3 = 4$, $k_4 = 200$, $k_5 = 2$, $k_6 = 50$. For the convenience of distinguishing, the simulation results under the controller proposed in this paper and PPC are marked with subscripts “a” and “b”, respectively.

Figures 4 and 5 illustrate the superior tracking performance of the proposed controller compared to PPC. While both controllers demonstrate acceptable transient tracking performance, PPC exhibits repetitive tracking errors of 30% of the initial error every 5 s in the longitudinal direction. Meanwhile, under PPC, the vertical channel of AUH experiences a negative overshoot of about 40% of the initial error at the beginning. It can be observed from Figs. 7 and 8, the occurrences of repetitive errors coincide with the high-amplitude peaks of pitch angular and control inputs. This suggests that neglecting the nonaffine structure in the control design may lead to significant repetitive tracking errors for the AUH, adversely affecting its safety in practical applications. In contrast, the proposed controller achieves a transient time of less than 2 s in both directions, maintaining tracking errors below 0.01 in the forward direction and zero error in the vertical direction. Furthermore, the proposed method effectively eliminates negative vibrations, enhancing its practical feasibility. The improved performance extends to other state variables as well. Figures 6 and 7 show that the proposed controller maintains these

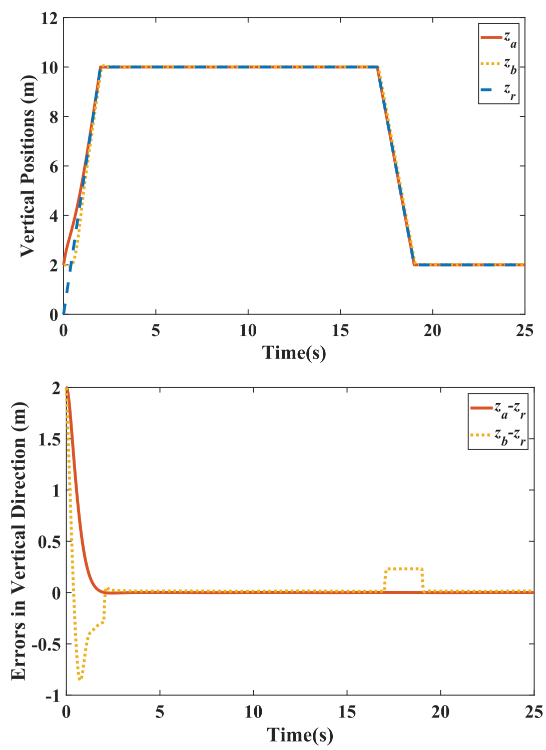

Fig. 5. Curves of vertical positions and tracking errors.

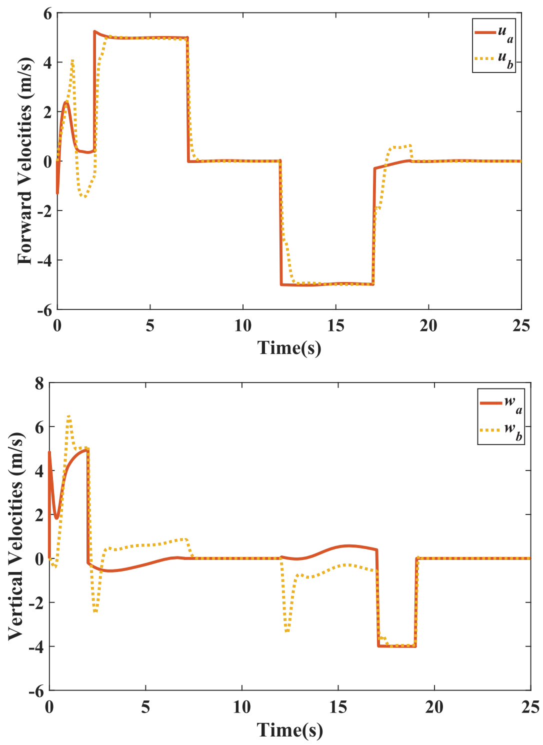

Fig. 6. Curves of forward and vertical velocities.

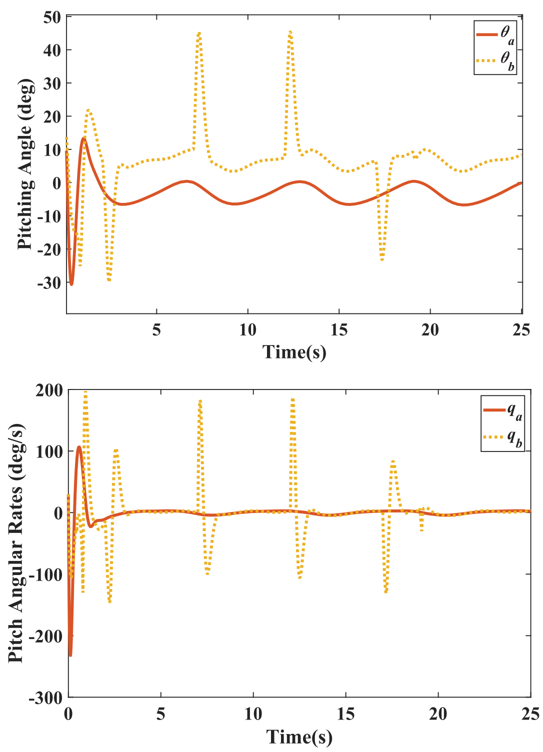

Fig. 7. Curves of pitching angles and angular rates.

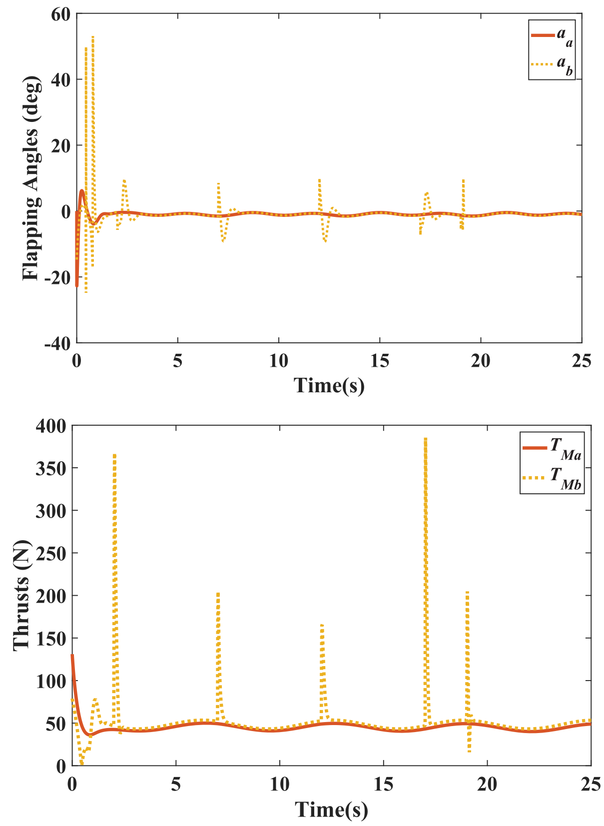

Fig. 8. Curves of flapping angles and thrusts.

states within a more desirable range compared to the PPC, which induces several peaks in the pitching angle and pitch angular rate. As depicted in Fig. 8, the proposed method keeps the control inputs within a reasonable range throughout the control process, implying safe and efficient operation of the AUH.

6. Conclusions

In this paper, we provide a novel control strategy for the disturbed 3-DOF AUHs with retained nonaffine structure and non-minimum phase character. The time-scale split is introduced by the designed flapping angle. Under SPT, the dynamics of AUHs are successfully decomposed into two subsystems in multiple time-scales. An observer-based controller is provided in the slow time-scale. The tracking performance and boundedness of all state signals are ensured by SPT. Comparative simulation results demonstrate the effectiveness and performance of the proposed method. Future research would extend this method to more general helicopter models and apply it to real-world helicopter platforms.

Acknowledgments

This research was supported by the National Key Research and Development Program of China (Grant No. 2023YFB4704900), the Aeronautical Science Foundation (Grant No. 20220056060001), the Scientific Instruments Development Program of NSFC (Grant No. 61527810), the Science and Technology Planning Project of Guangzhou, China (Grant No. 202201011133), the Natural Science Foundation of Guangdong Province (Grant No. 2024A1515011785), the Fundamental Research Funds for the Central Universities, and the Talent Project of Guangdong Polytechnic Normal University (Grant No. 2021SDKYA028).

References

[1] C. Zou, L. Li, G. Cai and R. Lin, Fixed-point landing method for unmanned aerial vehicles using multi-sensor pattern detection, *Unmanned Syst.* **12**(1) (2024) 173–182.

[2] J. Hu, H. Zhang, Z. Li, C. Zhao, Z. Xu and Q. Pan, Object traversing by monocular UAV in outdoor environment, *Asian J. Control* **23**(6) (2021) 2766–2775.

[3] J. Pravitra and E. N. Johnson, Development and flight testing of guidance, navigation, control, and operator interface for shipboard helicopter operations, *Unmanned Syst.* (2024) 1–16.

[4] J. Lee, J. Seo and J. Choi, Output feedback control design using extended high-gain observers and dynamic inversion with projection for a small scaled helicopter, *Automatica* **133** (2021) 109883–109896.

[5] L. Chen, T. Li, L. Liu and Z. Mao, Trajectory tracking anti-disturbance control for unmanned aerial helicopter based on disturbance characterization index, *Control Theory Technol.* **21**(2) (2023) 233–245.

[6] S. M. Schlanbusch and J. Zhou, Adaptive predictor-based control for a helicopter system with input delays: Design and experiments, *J. Autom. Intelli.* **3**(1) (2024) 50–56.

[7] M. Wan, M. Chen and K. Yong, Adaptive tracking control for an unmanned autonomous helicopter using neural network and disturbance observer, *Neurocomputing* **468** (2022) 296–305.

[8] Y.-C. Lai and T.-Q. Le, Adaptive learning-based observer with dynamic inversion for the autonomous flight of an unmanned helicopter, *IEEE Trans. Aerosp. Electron. Syst.* **57**(3) (2021) 1803–1814.

[9] A. Siddarth and J. Valasek, Tracking control for a non-minimum phase autonomous helicopter, in *AIAA Guidance, Navigation, and Control Conf.*, 2012, pp. 4453–4470.

[10] H. Yang and H. Pei, Two time-scale assignment with state extension for an autonomous helicopter, *Asian J. Control* **23**(4) (2021) 1707–1719.

[11] K. Yan, H. Chen, C. Chen, S. Gao and J. Sun, Time-varying gain extended state observer-based adaptive optimal control for disturbed unmanned helicopter, *ISA Trans.* **148** (2024) 1–11.

[12] J. Seo, S. Lee, J. Lee and J. Choi, Nonaffine helicopter control design and implementation based on a robust explicit nonlinear model predictive control, *IEEE Trans. Control Syst. Technol.* **30**(2) (2022) 811–818.

[13] K. P. Tee, S. S. Ge and F. E. Tay, Adaptive neural network control for helicopters in vertical flight, *IEEE Trans. Control Syst. Technol.* **16**(4) (2008) 753–762.

[14] W. Yan, J. Huang and D. Xu, Adaptive fuzzy tracking control for non-affine nonlinear yaw channel of unmanned aerial vehicle helicopter, *Int. J. Adv. Robot. Syst.* **14**(1) (2016) 1–12.

[15] Q. Zhang, X. Chen and D. Xu, Adaptive neural fault-tolerant control for the yaw control of UAV helicopters with input saturation and full-state constraints, *Appl. Sci.* **10**(4) (2020) 1404–1424.

[16] Z. Zhang, W. Li and S. S. Ge, Static gain function-based adaptive control for nonlinear systems with unknown time delays, *IEEE Trans. Autom. Control* (2023) 1–8.

[17] M. Mohammadzahri, A. Khaleghifar, M. Ghodsi, P. Soltani and S. AlSulti, A discrete approach to feedback linearization, yaw control of an unmanned helicopter, *Unmanned Syst.* **11**(1) (2023) 57–66.

[18] N. Hovakimyan, E. Lavretsky and C. Cao, Dynamic inversion for multivariable non-affine-in-control systems via time-scale separation, *Int. J. Control* **81**(12) (2008) 1960–1967.

[19] M. Asadi, H. T. Shandiz and A. Khayatian, Time scale separation in control of a single-link flexible-joint robot manipulator, *IMA J. Math. Control Inform.* **35**(2) (2018) 357–373.

[20] S. Yoo, Adaptive control of non-linearly parameterised pure-feedback systems, *IET Control Theory Appl.* **6**(3) (2012) 467–473.

[21] H. K. Khalil and J. W. Grizzle, *Nonlinear Systems* (Prentice hall Upper Saddle River, NJ, 2002).

[22] S. Wang, Approximation-free control for nonlinear helicopters with unknown dynamics, *IEEE Trans. Circuits Syst. II: Exp. Briefs* **69**(7) (2022) 3254–3258.

[23] D. M. Jeong and S. J. Yoo, Adaptive event-triggered tracking using nonlinear disturbance observer of arbitrarily switched uncertain nonlinear systems in pure-feedback form, *Appl. Math. Comput.* **407** (2021) 126335–126353.

[24] M. Chen and S. S. Ge, Adaptive neural output feedback control of uncertain nonlinear systems with unknown hysteresis using disturbance observer, *IEEE Trans. Indust. Electron.* **62**(12) (2015) 7706–7716.

[25] H. Min, S. Xu, Q. Ma, B. Zhang and Z. Zhang, Composite-observer-based output-feedback control for nonlinear time-delay systems with input saturation and its application, *IEEE Trans. Indust. Electron.* **65**(7) (2017) 5856–5863.

[26] Q. Zhou, P. Shi, S. Xu and H. Li, Adaptive output feedback control for nonlinear time-delay systems by fuzzy approximation approach, *IEEE Trans. Fuzzy Syst.* **21**(2) (2012) 301–313.

[27] H. Yang and H. Pei, A novel redesign framework to extend the application scope of a class of disturbance-rejection algorithms, *Int. J. Robust Nonlinear Control* **30**(1) (2020) 321–337.

[28] S. S. Ge and C. Wang, Adaptive NN control of uncertain nonlinear pure-feedback systems, *Automatica* **38**(4) (2002) 671–682.

[29] Y. Tan and L. Wu, Neuro-adaptive practical prescribed-time control for pure-feedback nonlinear systems without accurate initial errors, *Int. J. Adapt. Control Signal Process.* **37**(4) (2023) 915–933.

[30] N. Wang, Z. Fu, F. Tao, S. Song and T. Wang, A simplified adaptive tracking control for nonlinear pure-feedback systems with input delay and full-state constraints, *Int. J. Adapt. Control Signal Process.* **35**(12) (2021) 2521–2536.

[31] J. Seo, J. Lee, E. Baek, R. Horowitz and J. Choi, Safety-critical control with nonaffine control inputs via a relaxed control barrier function for an autonomous vehicle, *IEEE Robot. Autom. Lett.* **7**(2) (2022) 1944–1951.

[32] Z.-X. Fan, A. C. Adhikary, S. Li and R. Liu, Disturbance observer based inverse optimal control for a class of nonlinear systems, *Neurocomputing* **500** (2022) 821–831.

Hao Yang is an associate professor at Guangdong Polytechnic Normal University in Guangzhou, China. He holds his B.S. and M.S. degrees from Shaanxi University of Science and Technology in 2010 and 2013, respectively. Yang obtained his Ph. D. from the School of Automation Science and Engineering at South China University of Technology in 2020. His research focuses on nonaffine control, unmanned aerial vehicles, singular perturbation theory, and intelligent control.

Haixiang Jiang is currently pursuing an M.S. degree in Automatic Control of Automation at Guangdong Polytechnic Normal University. He received his B.S. degree from the North China Institute of Science and Technology in 2020. Research interests include singular perturbation theory, optimal control, and nonlinear control.

Hailong Pei is a professor at the School of Automation Science and Engineering, South China University of Technology. He received his Ph.D. in Automatic Control from the same institution in 1992 and completed postdoctoral research at the Chinese University of Hong Kong from 1997 to 1998. Professor Pei specializes in robot control, neural networks, and nonlinear control.

Xinpan Gou obtained his B.S. degree in Automation and Electrical Engineering from Chengdu Technological University in 2021. He subsequently earned his M.S. degree in Automatic Control from Guangdong Polytechnic Normal University in 2024. Gou's research interests encompass singular perturbation theory, adaptive control, and methods for delayed systems.